European Journal of Echocardiography (2010) **11**, 81–96
doi:10.1093/ejechocard/jep234

REVIEW PAPER

The echocardiographic assessment of the right ventricle: what to do in 2010?

Ruxandra Jurcut[1]*, Sorin Giusca[1,2], André La Gerche[2], Simona Vasile[1], Carmen Ginghina[1], and Jens-Uwe Voigt[2]

[1]Department of Cardiology, University of Medicine and Pharmacy 'Carol Davila', Bucharest, Romania; and [2]Department of Cardiology, Catholic University Leuven, Leuven, Belgium

Received 17 August 2009; accepted after revision 28 December 2009; online publish-ahead-of-print 2 February 2010

For many years, the echocardiographic quantitative assessment of right ventricular (RV) function has been difficult owing to the complex RV anatomy. Identifying an accurate and reliable echocardiographic parameter for the functional assessment of the RV still remains a challenge. The review presents a summary of the most studied and presently used parameters of RV function, with their reported normal values, as well as advantages and limitations of use. Combinations of these parameters are used in daily clinical practice, each one offering only partial information about the status of the RV. Myocardial velocity and strain rate imaging have promising results in the assessment of RV function. There is hope that novel myocardial deformation parameters and three-dimensional echocardiography-derived parameters may add value to the examination of the RV, but validation studies are still needed.

Keywords Right ventricle • Echocardiography • Tissue Doppler • Strain rate imaging • 3D echocardiography

Introduction

For decades, the right ventricle (RV) has been considered 'dispensable' for cardiac function and consequently ignored. The introduction of the Fontan procedure for complex congenital heart disease in 1968, a technique that directly connects the right atrium to the pulmonary artery, thus 'bypassing' the RV, cemented this belief. Only in the second half of the past century, after recognizing its key role in various physiological[1] and pathological conditions,[2–5] the RV regained attention. The RV performance defines prognosis in patients with congenital heart disease.[2] In this population group, the RV may be subjected to either volume (atrial septal defect, pulmonary, and/or tricuspid regurgitation) or pressure overload (pulmonary stenosis, atrial switch operations, congenitally corrected transpositions). Assessing RV morphology and function is of paramount importance in acquired diseases as well. The RV has a great impact on the prognosis of patients with pulmonary hypertension, myocardial infarction involving the RV, and left ventricular (LV) dysfunction.[5,6]

Echocardiography, being non-invasive, widely available, relatively inexpensive, and having no side effects, is the modality of choice for the assessment of morphology and function of the RV in clinical practice. Recent developments have provided several new methods for analysing the RV, each having advantages and disadvantages. Doppler myocardial imaging (DMI), speckle tracking, or 3D echocardiography (3D Echo) are some of the techniques that may now add to a better understanding of RV function.

In this article, we review the currently available echocardiographic techniques and parameters for RV assessment in clinical practice and for research purposes, with a focus on acquired heart diseases.

Anatomy and physiology of the right ventricle

The RV is positioned directly behind the sternum, anterior to the left ventricle (LV). It has a complex geometry, appearing triangular when viewed from the front, and crescentic when viewed in a transverse section of the heart, with the septum being the most important determinant of shape. Under normal loading conditions, the septum arches into the RV both in systole and diastole. This complex geometry cannot be fitted to simple geometric models, which presents important limitations for the estimation of RV volume and function based on two-dimensional (2D) tomographic views.

In a normally developed RV with atrioventricular and ventriculoarterial concordance and normal tricuspid and pulmonary valves, three anatomical parts of the RV can be distinguished: the inlet part which accommodates the tricuspid valve, the trabeculated apical

* Corresponding author. Department of Cardiology, Institute of Emergency for Cardiovascular Diseases 'Prof. Dr. C.C.Iliescu', Sos.Fundeni no. 258, 022322 Bucharest, Romania. Tel/Fax: +40 21 3175227. Email: rjurcut@gmail.com

part, and the outlet.[7,8] The myocyte arrangement in the RV wall differs from that of the three-layered LV. Myocytes are predominantly oriented in the longitudinal direction in the subendocardial layer. Circumferentially oriented myocytes are found in the thinner subepicardium.[9] Consequently, the RV contraction pattern is predominantly longitudinal.[10,11] Studies report a sequence of contraction during ejection that can be recognized first at the apex and propagates towards the outflow tract.[12] To further differentiate the RV from the LV, rotational deformation plays only a minor role in RV contraction.

The thickness of the RV free wall is in the range of only 3–5 mm,[13,14] and the RV mass is approximately one-fourth of that of the LV.[15,16] Still, owing to the lower impedance and greater distensibility of the pulmonary artery bed, the RV can pump blood at the same rate and volume as the LV.

The ability of both ventricles to maintain a normal cardiac output, ensuring sufficient organ perfusion, depends on three key factors: the contractile status of myocardial tissue, the pre-load, which represents the initial stretching of cardiac myocites prior to contraction, and the afterload, defined as the load against which the heart must contract to eject blood.[17] In addition, RV performance is directly influenced by LV functional status owing to ventricular interaction.[18] The interventricular septum, the pericardium, and common muscle fibres all play an important role in facilitating the transfer of force from the LV to the RV during the cardiac cycle.[19] Around one-third of the pressure generated in the RV is determined by LV contraction.[20] This direct influence of the LV was also proved by animal experiments where the RV free wall was replaced with a non-contractile patch without any measurable haemodynamic deterioration.[21]

Right ventricular function is susceptible to elevated afterload, with a small range of pressure against which it can maintain a normal cardiac output.[6] In contrast, it better tolerates volume overload which alters RV geometry, but does not influence the pattern of ejection.[22]

The particular haemodynamic environment of the right heart has direct implications on the phases of the cardiac cycle in the RV. Under normal circumstances, the low end-diastolic pressure in the pulmonary artery is quickly exceeded by the pressure rise in the RV, resulting in a very short or even absent isovolumic contraction time.[23] Another element that separates RV from LV physiology is the existence of a 'hang-out' period during ejection. In this time interval during RV pressure fall until pulmonary valve closure,[24] ejection of blood is maintained most likely as a consequence of the high capacitance of the pulmonary circulation which allows the preservation of blood momentum. Similar to the isovolumic contraction, isovolumic relaxation is very short or may even be absent under normal conditions,[23] the corollary being that a measurable isovolumic relaxation time (IVRT) is an indicator of elevated end-systolic RV pressure.

Pathophysiology of the right ventricle

Intrinsic contractile dysfunction, a change in loading conditions beyond physiological limits, as well as an altered performance of the LV can all have detrimental effects on RV function.

Right ventricular myocardial ischaemia or infarction is the major primary cause of RV contractile dysfunction. The RV is affected in 50% of inferior infarctions.[25] Other primary RV myocardial diseases such as arrhythmogenic RV cardiomyopathy (ARVC) can be associated with globally or regionally decreased RV performance.[26]

An acute change in afterload of sufficient magnitude, as produced by pulmonary embolism (PE), can quickly result in RV failure as the RV has little ability to cope with this condition.[27] A chronic exposure to an increased afterload results in RV hypertrophy and altered geometry, which temporarily reduces wall stress but ultimately results in RV failure.[28] In addition, the flattening or displacement of the IVS seen in chronic RV pressure overload impairs LV compliance and filling.[29] The mechanisms leading to RV failure in patients with chronic pulmonary hypertension are not fully understood. Potential mechanisms are: RV myocardial ischaemia, altered inflammatory and oxidative stress, abnormalities in endothelin and nitric oxide systems, and myocyte apoptosis. The time of occurrence of increased afterload may also influence RV response. As shown in a recent pilot study, patients with congenital pulmonary stenosis perform better than those with acquired pulmonary hypertension despite a comparable degree of RV afterload (R. Jurcut *et al.*, personal communication).

Volume overload is a condition which is better tolerated by the RV, but, if sustained, will also ultimately lead to RV functional decline.[2]

Left ventricular failure may directly impact on RV function by ventricular interaction in that an exaggerated displacement of the septum into the RV may impair both filling and contractility of the RV.

Echocardiographic evaluation of the right ventricle

General considerations

Echocardiographic assessment of the RV is complicated by the complex geometry of this chamber, the pronounced trabeculation that compromises accurate endocardial delineation, and the anterior position that often limits echo image quality.[30] Owing to the incomplete visualization of the RV in a single 2D echocardiographic view, more than one projection is needed for a comprehensive evaluation of RV structure and function[13,31,32] (*Figure 1*, *Table 1*).

In case of uncertainty (e.g. in congenital disease), several morphological features help to identify the RV: the more apical position of the tricuspid valve compared with the anterior mitral valve, coarse apical trabeculations, the presence of a moderator band, and the presence of septal papillary attachments for the tricuspid valve.[33]

Right ventricular morphology

A qualitative evaluation of the RV can be obtained by assessing the shape of the RV, which can be visualized in a parasternal short-axis view. When the RV is overloaded, the crescent shape is lost and the septum becomes flat, the LV taking the shape of the letter 'D', resulting in an impaired LV filling and a decrease in cardiac

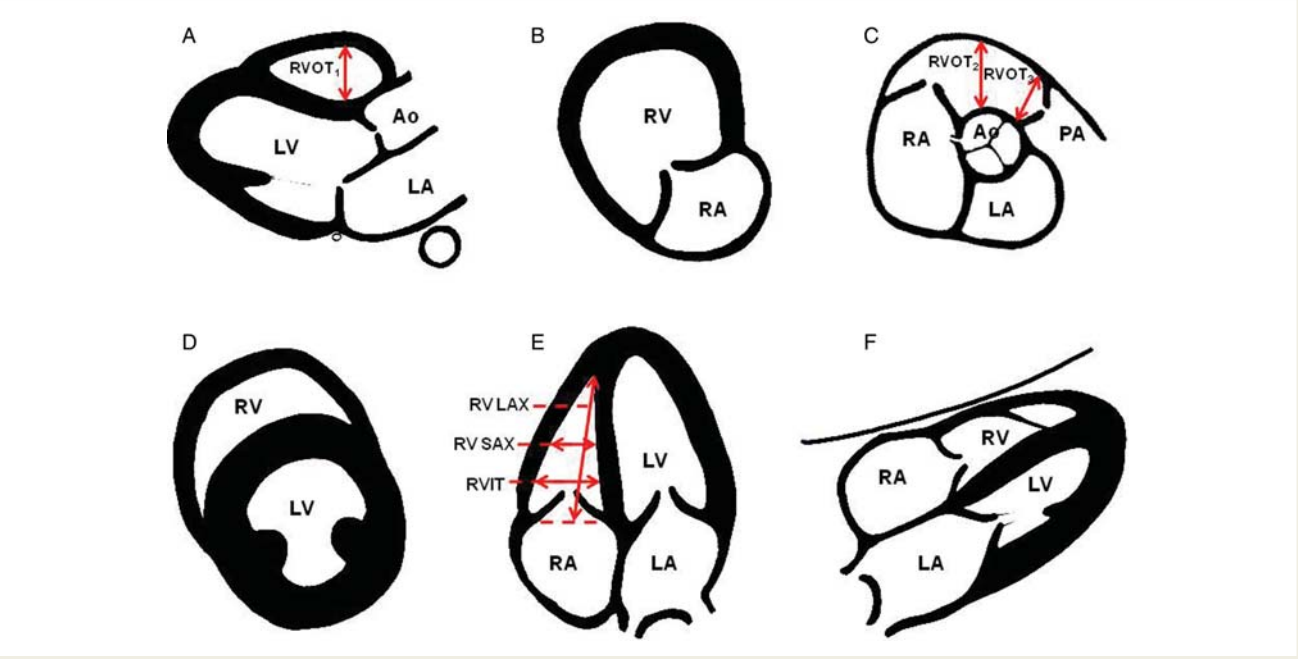

Figure 1 Graphic representation of the echocardiographic views used for evaluating the right ventricle. (*A*) Parasternal long-axis view; (*B*) long-axis view of the inflow tract; (*C*) parasternal short-axis view at the base of the heart; (*D*) parasternal short-axis view at the level of the papillary muscles; (*E*) apical four-chamber view; (*F*) subcostal view. Legend: Ao, aorta; LA, left atrium; LV, left ventricle; PA, pulmonary artery; RA, right atrium; RV, right ventricle; RVIT, RV inflow tract; RV LAX, RV long axis; RV SAX, RV short axis; RVOT, RV outflow tract.

Table 1 Echocardiographic sections for right ventricle evaluation

Echocardiographic section	Recommended measurements
Parasternal long axis	End-diastolic diameter of RVOT (2D, M-mode)
Long-axis view of the RV inflow tract (modified parasternal long axis)	Anatomy and function of the tricuspid valve (posterior and anterior cusps)
RV outflow tract view (modified parasternal long axis)	Pulmonary valve
Parasternal short axis—base of the heart	End-diastolic and end-systolic diameters of the RV outflow tract RVOT shortening fraction
Parasternal short axis—papillary muscles level	LV eccentricity index
Apical four-chamber view	RV long and short-axis diameters TAPSE RV fractional area change Tricuspid valve (anterior and septal cusps)
Subcostal view	RV free wall thickness

LV, left ventricle; RVOT, right ventricular outflow tract; RV, right ventricle; TAPSE, tricuspid annulus plane systolic excursion (after Lang *et al.*[13] and Ho and Nihoyannopoulos[31]).

output. The pattern of movement displayed by the septum in systole and diastole can help distinguish between volume overload and pressure overload.[34] In conditions characterized by RV volume overload, the flattening of the septum is seen only in diastole, the septum regaining its normal shape in systole. When the RV is subjected to a pressure overload, the septum will move towards the RV in systole in a first stage, maintaining the altered shape during the entire cardiac cycle when the condition aggravates (*Figure 2*). Based on interventricular interaction, changes in RV shape can be characterized by the LV eccentricity index (EccIx), defined as the ratio of the LV antero-posterior to septo-lateral diameters in a short-axis view (*Figure 3*), and can be measured at both end systole and end diastole. Normal individuals have a value of 1 in both systole and diastole (the LV being approximately circular in transverse sections). A value higher than 1 at end diastole suggests RV volume overload and a value above 1 at end systole and end diastole is highly suggestive for RV pressure overload.[35]

As estimating the volume of a complex structure like the RV is challenging, not allowing any geometrical assumptions, diameters and areas are used as surrogate in 2D Echo. Although the segment of the RV visualized in a parasternal long-axis view is neither the true RV outflow tract (RVOT) nor the true inflow

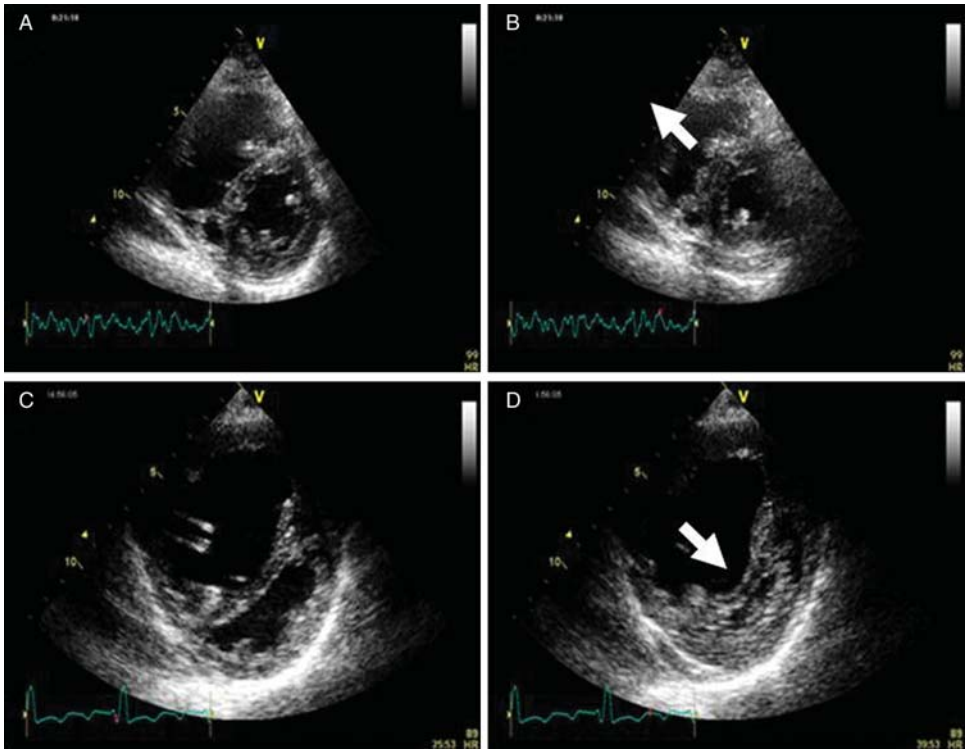

Figure 2 Parasternal short-axis views at the mid-ventricular level. (*A* and *B*) Patient with atrial septal defect type ostium secundum, consequent right ventricular volume overload, and mildly elevated pulmonary artery pressures—flattening of the interventricular septum at end diastole (*A*) and recovering of shape at end systole (arrow) (*B*). (*C* and *D*) Patient with severe pulmonary arterial hypertension and consequent severe right ventricular pressure overload—flattening of the interventricular septum both at end diastole (*C*) and end systole (arrow) (*D*).

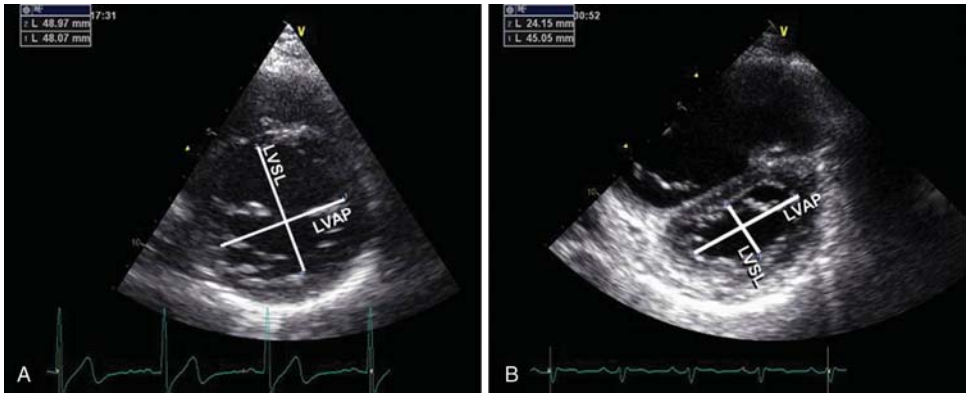

Figure 3 Parasternal short-axis views at the mid-ventricular level illustrating measurements of left ventricular diameters for calculation of the eccentricity index (EccIx). (*A*) Normal heart with diastolic EccIx = 1. (*B*) Patient with pulmonary hypertension with diastolic EccIx = 1.8. Legend: LVAP, LV antero-posterior diameter; LVSL, LV septo-lateral diameter.

part, determining the RV diameter in this view with a perpendicular line on the septum was proved more reproducible and less variable than the RVOT diameter measured in a parasternal short-axis view[31] (*Figure 1A* and *C*). In a multicentre study, to compare findings in patients with ARVC and normal controls, an increased RVOT diastolic diameter, irrespective of the view in which it was measured, was the most common finding in probands.[36] The diameter of the RVOT can be measured in the parasternal short-axis views, proximal to the pulmonary valve, as well as from a modified parasternal long-axis view angled superiorly.[13]

In an apical four-chamber view, both the long- and short-axis diameters can be measured and the end-systolic and end-diastolic

areas can be determined.[37] In normal individuals, RV area and mid-cavity diameter should be smaller than those of the LV, thus allowing a simple visual assessment of RV area.

Assessment of the structure and architecture of the RV walls can identify features which suggest a particular aetiology, such as RV infarct or ARVC. For instance, the presence of localized RV free wall aneurysms is a major diagnostic criteria for ARVC, while a high degree of trabeculation, increased thickness of the moderator band with a hyperechogenic appearance, and RVOT dilatation can also support this diagnosis.[38] However, on the basis of visual echocardiographic assessment solely, identification of functional abnormalities is inaccurate, frequently resulting in false-positive findings,[26,39] and newer echocardiographic techniques help in a more accurate evaluation.

The maximum limit for normal thickness in the RV free wall is 5 mm,[31] above which the ventricle is considered to be hypertrophied. Right ventricular hypertrophy can be seen in various pathological states: RV pressure overload, biventricular hypertrophic cardiomyopathies, and deposit diseases. For RV mass quantification, real-time 3D echocardiography (RT3DE) is superior to 2D Echo,[40] and post-processing of full-volume datasets can lead to LV mass and volume calculation.[41] The excellent accuracy and reproducibility of cardiac magnetic resonance imaging (MRI) is well established, making MRI a gold standard technique in quantifying the RV chamber.[16,42,43] However, it remains confined to experienced centres and involves high costs. Several studies showed good correlations between RT3DE and MRI-measured RV volume, ejection fraction, and mass.[40]

Assessment of right ventricular function

Global right ventricular function

Standard parameters

Unlike the LV, where biplane methods are accepted and widely used for a global assessment of systolic function, a quantitative approach towards evaluating RV global function is more difficult to achieve owing to its more complex shape.[44] Therefore, surrogate parameters were developed and were further validated against ejection fraction derived using isotopic methods or MRI.

Right ventricular outflow tract shortening fraction (RVOT-SF) is obtained from a parasternal short-axis view at the base of the heart where the end-diastolic RV outflow tract diameter (EDRVOTD) and end-systolic RVOT diameter (ESRVOTD) can be measured and the shortening fraction is calculated using the formula: RVOTSF (%) = (EDRVOTD − ESRVOTD)/EDRVOTD (*Figure 4A*). Lindqvist *et al.*[45] found that RVOT fractional shortening correlates well with longitudinal function, pulmonary pressure gradient, and RV-right atrial (RA) pressure gradient. Care must be taken when measuring this parameter, as there are no defined landmarks for orientating the image with precision, and thus significant inaccuracies may result from oblique plane acquisitions.

Right ventricular fractional area change (RVFAC) expresses the percentage change in RV area between end-diastole and end-systole. It is obtained from a four-chamber view where the RV end-diastolic (RVEDA) and end-systolic areas (RVESA) are measured, and the RVFAC is calculated as follows: RVFAC (%) = (RVEDA − RVESA)/RVEDA (*Figure 4B*). It has a good correlation with MRI-derived RVEF and was shown to have prognostic significance in patients with myocardial infarction and pulmonary hypertension.[46–48] Its main limitation is related to the need of good endocardial border delineation, which can be difficult to achieve in the highly trabeculated RV.

Tricuspid annular plane systolic excursion (TAPSE) has proved a useful index for evaluating RV longitudinal function. It is especially attractive in clinical practice given the ease with which it is measured using an M-mode cursor passed through the tricuspid lateral annulus in a four-chamber view (*Figure 5A* and *B*). This parameter measures the extent of systolic motion of the lateral portion of the tricuspid ring towards the apex. It has been shown to have a good correlation with isotopic derived RVEF,[37] although Anavekar *et al.*[49] failed to find any correlation between TAPSE and MRI-derived ejection fraction. Normal values for TAPSE are 15–20 mm. The prognostic value of TAPSE was emphasized in cardiac failure and myocardial infarction.[50,51] Samad *et al.*[52] assessed TAPSE in patients after a first acute myocardial infarction, and showed that TAPSE $\leq$15 mm was associated with increased mortality (45% at 2 years) compared with patients having TAPSE $>$20 mm (4%). Although simple to use, TAPSE has some inherent limitations mostly because assessment is restricted to the longitudinal function of the RV free wall, disregarding the contribution of the interventricular septum and the RVOT.[53] As TAPSE is measured relative to transducer position and was shown to be influenced by the functional status of the LV,[54] care must be taken when interpreting this parameter in longitudinal studies of patients undergoing procedures that affect the overall heart motion (cardiac surgery).[55]

The myocardial performance index (MPI, Tei index) differs from the previously described parameters in that it is derived from physiological rather than structural features. It is calculated as the ratio between the sum of the times of the isovolumic periods and the ejection time for the RV.[56] The MPI is a parameter of global function, combining information on both systole and diastole. Unlike the left heart, where these time intervals can be determined during the same cardiac cycle (owing to the possibility of aligning the mitral and the aortic valves in the same view), measuring MPI for the right heart using conventional Doppler techniques is less accurate, as it needs at least two different cardiac beats for determining the time periods. The ejection time can be determined from the parasternal short-axis view at the pulmonary valve, while isovolumic intervals are derived based on the tricuspid flow. Myocardial performance index was shown to correlate with radionuclide-derived RVEF.[57] Normal values for MPI are 0.28 ± 0.04, and it usually increases in diseases associated with RV dysfunction.[58] Furthermore, it was shown to be useful in the longitudinal follow-up of patients with chronic thrombo-embolic pulmonary hypertension who undergo pulmonary thrombendarterectomy, in whom RV MPI decreases after treatment.[59,60] However, the use of this index is limited by the absence of the isovolumic periods in the normal RV as well as the pseudonormalization of the index when RA pressure is increased as shown by Yoshifuku *et al.*[61] (*Figure 6*). The increased RA pressure determines a shortening of the IVRT that will result in a decreased value of the MPI index.

Another parameter of contractility is RV d*P*/d*t* measured on the tricuspid regurgitation envelope. Although it was shown to be highly load-dependent and not reflecting the contractile status of

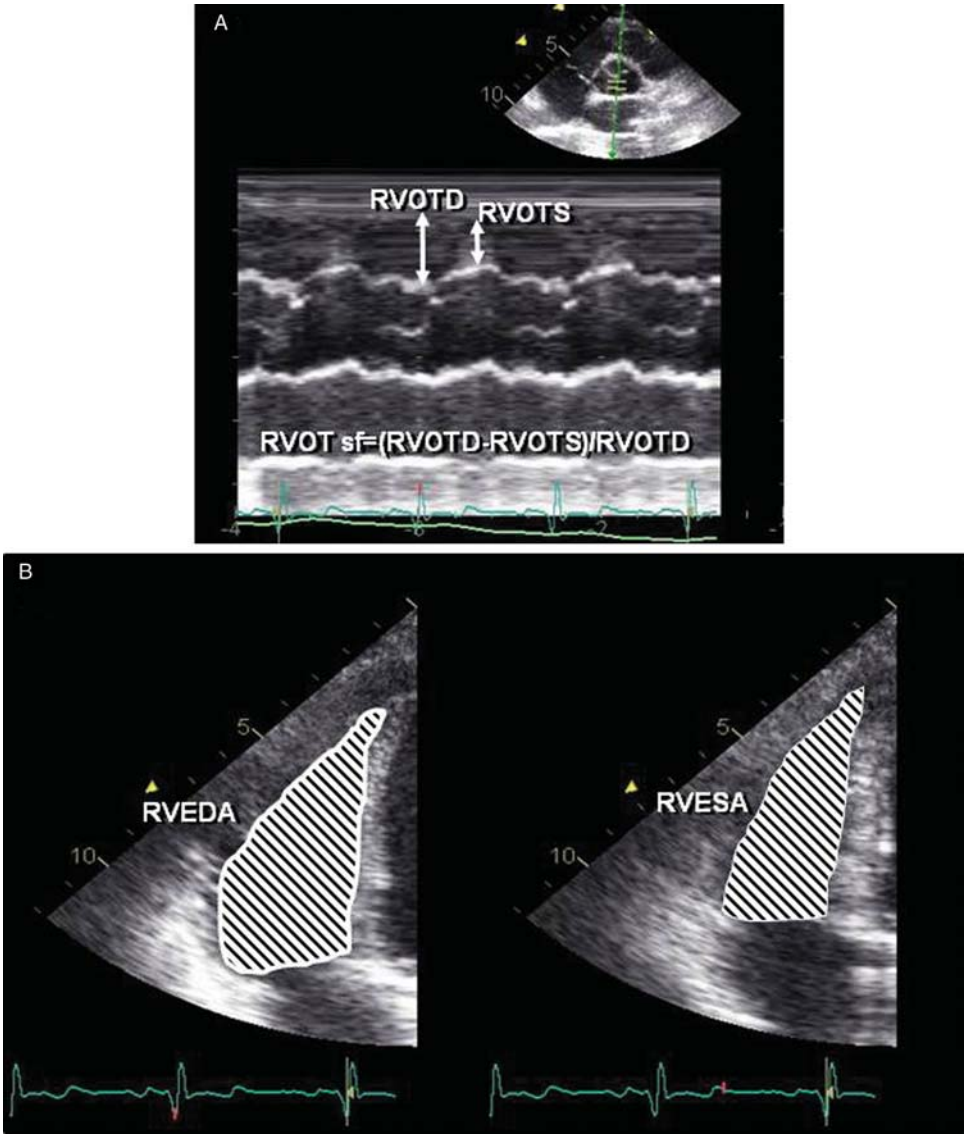

Figure 4 Methods of determining indices of right ventricular systolic function. (*A*) Determining right ventricular outflow tract shortening fraction (RVOT-SF) as a ratio between the difference in end-diastolic (RVOTD) and end-systolic (RVOTS) diameter and RVOTD. (*B*) Measurements of right ventricular end-diastolic area (RVEDA) and right ventricular end-systolic area (RVESA), from which right ventricular fractional area change is derived as 100*(RVEDA − RVESA)/RVEDA (%).

the RV muscle, it may still be useful for repeated longitudinal assessments.[32,62]

Novel methods

Doppler myocardial imaging is a technique that offers information on myocardial velocities, allowing a quantitative assessment of myocardial function during the entire cardiac cycle. Using DMI, several global and regional parameters, such as timing, direction, amplitude of the velocity of the ventricular wall can be determined. Being a Doppler-based technique, alignment with the ultrasound beam is very important, an improper alignment (>20°) yields erroneous results. The technique is less dependent on chamber geometry, but a good alignment of the ultrasound beam with the interrogated wall becomes increasingly difficult in dilated ventricles. Furthermore, no endocardial border delineation is needed, which makes DMI usable even if the echocardiographic image quality is suboptimal.

Pulsed DMI is simple to use online and has a very good temporal resolution. Meluzin *et al.*[63] found that a cut-off value of 11.5 cm/s for tricuspid ring systolic velocities is able to accurately predict global RV dysfunction (defined as RVEF <45%). Apart from angle dependency, the main disadvantage is that the sample volume is fixed and does not enable tracking of the region of interest as it translates with the cardiac cycle and respiration.

Colour DMI is an alternative to pulsed DMI. It allows an offline analysis of several myocardial segments during the same cardiac cycle. Sample volumes can be set to follow cardiac motion. Colour DMI values represent the median of the velocity spectrum

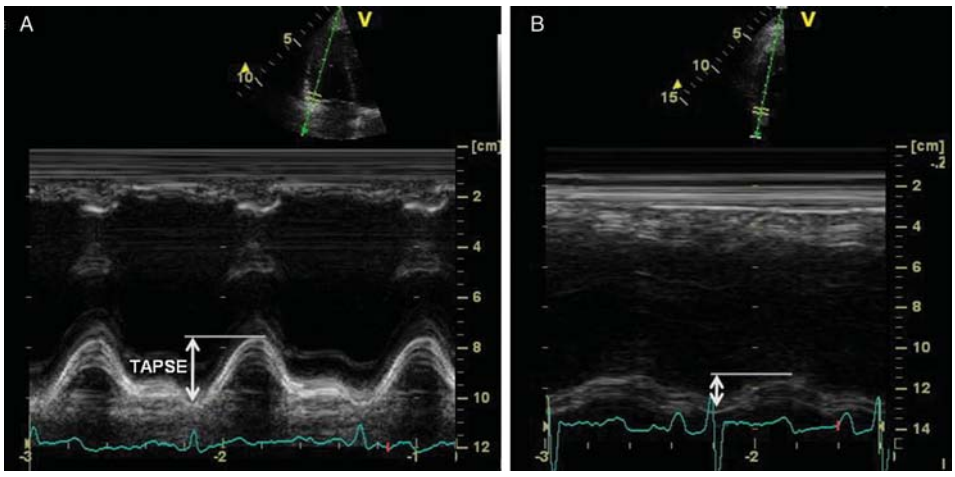

Figure 5 Measurements of tricuspid annular plane systolic excursion (TAPSE) in a normal individual −24 mm (*A*) and in a patient with pulmonary hypertension −9 mm (*B*).

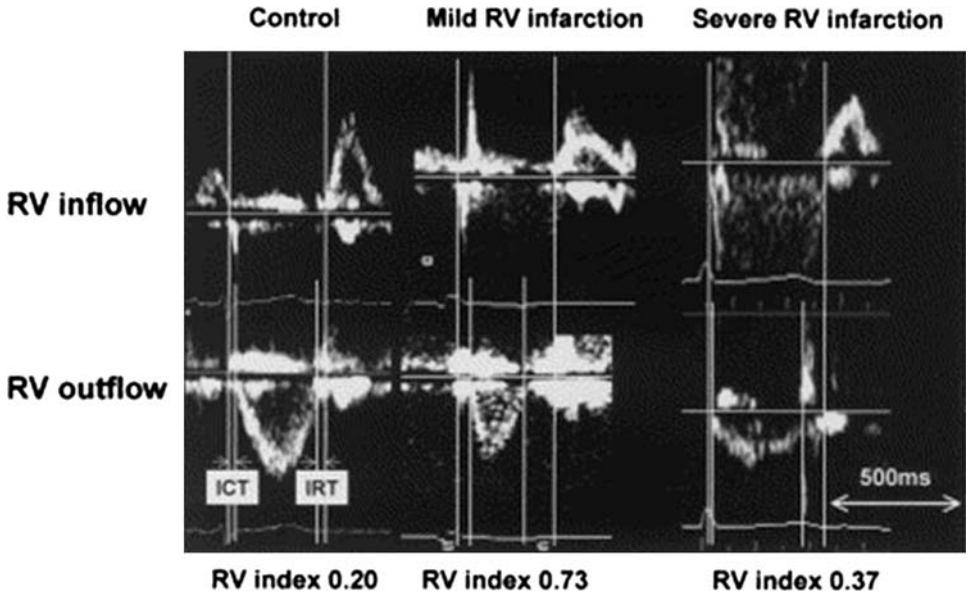

Figure 6 Pseudonormalization of the right ventricular Tei index—representative patients. Left panel: a control subject with normal isovolumic contraction time (ICT) and isovolumic relaxation time (IRT). Middle panel: this patient had mild/moderate right ventricular infarction and a larger Tei index with prolonged ICT and IRT. Right panel: this patient had severe right ventricular infarction with paradoxic shortening of ICT, resulting in a pseudonormalized right ventricular Tei index. Reproduced with permission from Yoshifuku *et al.*[61]

and are around 25% lower than those obtained using pulsed DMI in which the maximal spectral velocity value is measured.[64] At frame rates of 150–160 fps, the temporal resolution is considered acceptable,[65] and with wall-by-wall acquisitions, the frame rate can be as high as 180–220 fps.

Parameters derived from tissue Doppler imaging (TDI) techniques which may aid in the estimation of global RV function are IVRT, Tei index, isovolumic myocardial acceleration.

A normal RV that functions with preserved contractility and under normal loading conditions does not have a measurable IVRT. The end of systolic movement is immediately followed by early filling. A pressure increase in the RV leads to a sustained prolongation of the IVRT. As a consequence, in patients where the alignment with the tricuspid regurgitant flow is suboptimal, measuring IVRT using TDI techniques can be an alternative for estimating pulmonary systolic pressure.[66,67]

The Tei index measured using DMI methods has the advantage of measuring the isovolumic periods in the same cardiac cycle (*Figure 7*).[68] A good correlation was obtained between the Tei index derived from DMI and conventional Doppler.[69]

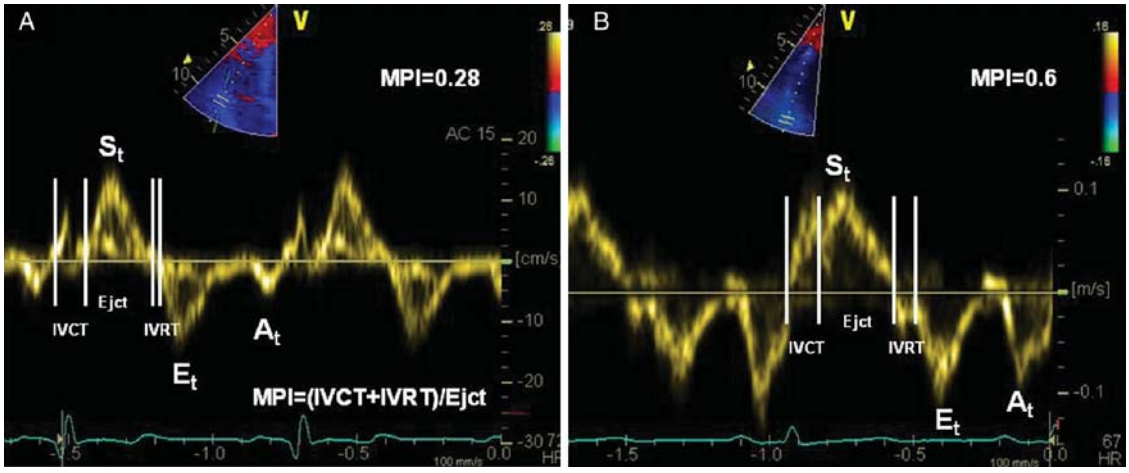

Figure 7 Pulsed-wave Doppler at the tricuspid level of the right ventricular free wall in a normal individual (*A*) and in a patient with pulmonary hypertension (*B*). MPI, myocardial performance index; IVRT, isovolumic relaxation time; IVCT, isovolumic contraction time; Ejct, ejection time; S_t, peak systolic velocity at the tricuspid valve; E_t, peak early filling velocity at the tricuspid ring; A_t, peak late filling (atrial) velocity at the tricuspid ring.

Moreover, DMI-derived parameters can differentiate between volume-overload and pressure-overload conditions, as shown by Hsiao *et al.*[70] They showed that in RV pressure-overload conditions, tricuspid ring velocities are lower and IVRT increases, as opposed to volume-overload conditions, where the ring systolic velocities increase significantly, whereas diastolic velocities decrease.

Myocardial isovolumic acceleration time (IVA) is a DMI-derived index that is supposed to be less dependent on loading conditions in a physiological range.[71,72] It is calculated as the ratio between maximum systolic velocity and time to maximum systolic velocity (*Figure 8*). Studies have shown that an IVA measured in the basal segment of the RV free wall of >1.1 m/s^2 correlates well with MRI RVEF $>45\%$ (90% sensitivity and specificity).[73] The value of this parameter was confirmed in congenital heart disease (e.g. in the transposition of the great arteries, repair of tetralogy of Fallot).[74,75] Concerns exist regarding its reproducibility and dependence on the temporal resolution of the underlying data.[76]

Three-dimensional echocardiography has emerged as the non-invasive technique that would overcome the geometric limitations of standard 2D Echo. Using this technique, volumes and, consequently, ejection fraction should be determined with high accuracy and without any geometrical assumptions (*Figure 9*). Similar acquisition techniques to 2D Echo are employed, but the visualization of the entire RV (especially the apical anterior wall and RVOT) remains a challenge—particularly in enlarged hearts in which the appraisal of RV function is especially relevant. Larger sector widths may be achieved when images are acquired over multiple cardiac cycles, but this can result in 'stitch artefacts' when there is cardiac motion owing to respiration or inconsistent cycle length owing to arrhythmias. Earlier studies have shown a weak correlation between 3D Echo-derived RVEF and MRI-derived RVEF,[77,78] although, in a more recent study, Niemann *et al.*[79] found an excellent correlation between 3D Echo- and MRI-derived RVEF. Measurements of RV volumes and RVEF by RT3DE have also proved feasible, accurate, and reproducible in children when compared with MRI measurements.[80] Despite these encouraging reports, further studies are needed to assess the technical aspects of acquiring data sets and to determine the range of RV volumes and RVEF in health and pathology.

Right ventricular regional function

Tissue velocities can be measured using pulsed or coloured DMI at three different levels of the RV free wall: basal, mid and apical.[81] Several groups only report two segments per RV free wall owing to anatomical (difficulties in accurately obtaining data from the apical segment) or physiological considerations (the basal segment representing the function of the smooth inlet component and the apical one representing the function of the trabeculated inlet component).[82]

Longitudinal and radial velocities recorded at the level of the RV free wall using colour TDI in normal individuals were shown to be higher than those measured in the LV.[81,83] Peak systolic velocities measured in the basal segment of the free RV wall have proved useful indices in the diagnosis and prognosis of patients with RV infarction,[84] patients with systolic annular velocities ≥ 8 cm/s having a significantly better event-free survival at 1 year than patients with systolic annular velocities <8 cm/s.

Doppler myocardial imaging based techniques allow not only for the evaluation of myocardial velocities but also for extracting myocardial deformation parameters (strain and strain rate). These parameters were already reported as useful for analysing global and regional functions in the LV[85,86] and also in detecting subtle changes in the myocardial functional status that would have been overlooked by standard echocardiography parameters.[87–89]

Strain (S)/strain rate (SR) represents deformation and deformation rate, respectively. Strain is defined as deformation of an object compared with its initial shape and is expressed as

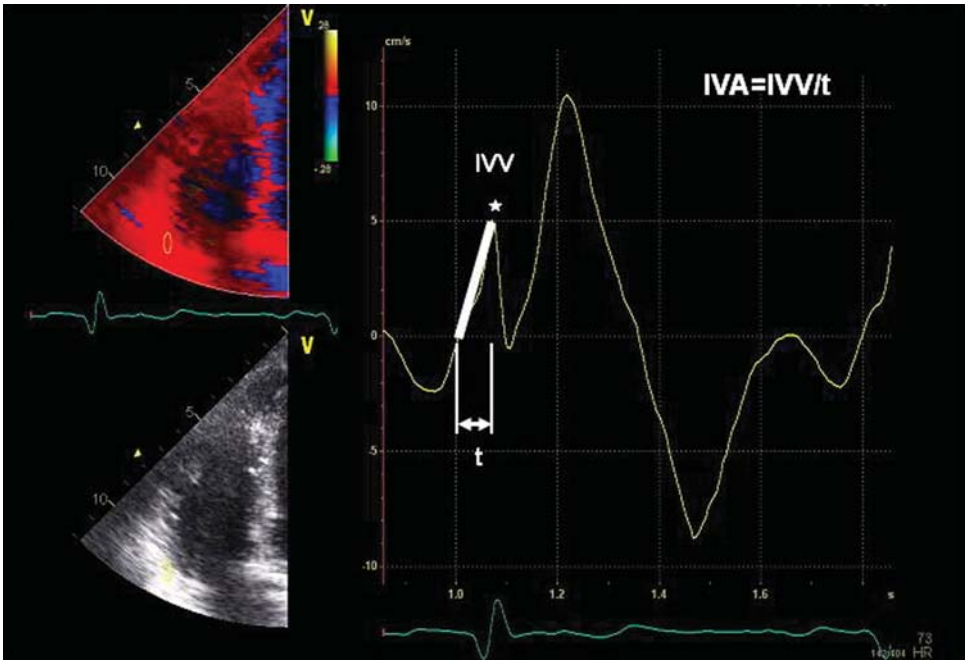

Figure 8 Measuring isovolumic acceleration (IVA) during isovolumic contraction at the basal segment of the right ventricular free wall. IVV, peak isovolumic velocity, *t*, time from zero crossing to peak isovolumic velocity.

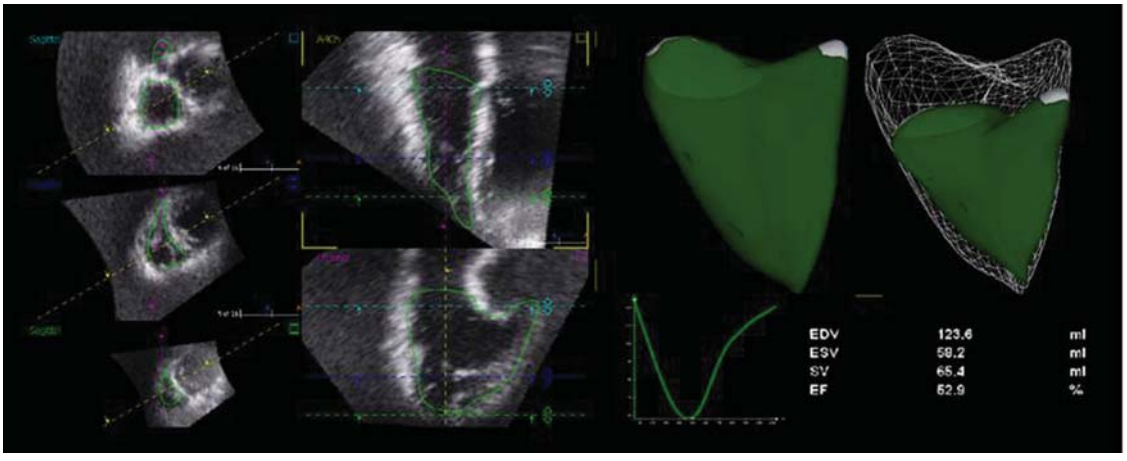

Figure 9 Three-dimensional imaging of the right ventricle with measurements of the right ventricular volumes and ejection fraction in a healthy individual.

percentage. By convention, shortening (and thinning) has a negative value, while lengthening (and thickening) has a positive value. In systole, S will have a negative value for longitudinal shortening and a positive value for radial thickening. End-systolic S was shown to correlate well with regional EF.[90] Strain rate or deformation rate defines the speed of the deformation, and correlates well with regional contractility parameters, providing information which is less dependent on the loading conditions.[91]

Longitudinal myocardial deformation parameters of the RV free wall were described in normal individuals,[87] athletes,[92] and subjects with pulmonary hypertension[82] or ARVC.[39] *Figures 10* and *11* illustrate both Doppler-derived and speckle-tracking-based strain curves in normal individuals and PHT patients.

With TDI techniques using a three segment model of the RV free wall in normal individuals, Kowalski *et al*. showed that S and SR recorded in the apical segment have the highest values as opposed to the distribution of velocities in which the highest values are measured in the basal segment. Furthermore, TDI-derived S and SR were used to describe RV function in patients with pulmonary hypertension.[82,93] Dambrauskaite *et al*.[82]

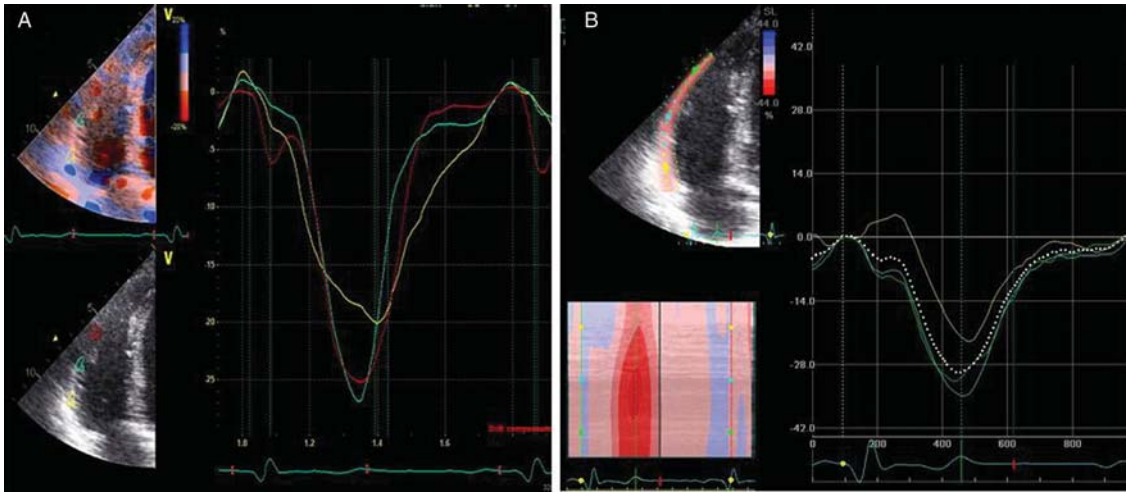

Figure 10 Strain measurements in the right ventricular free wall of a normal individual using tissue Doppler techniques (*A*) and speckle-tracking techniques (*B*).

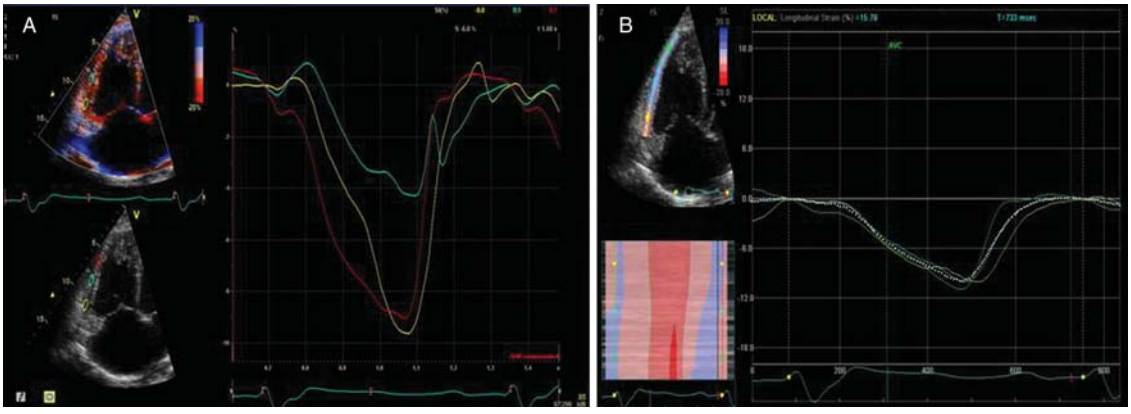

Figure 11 Strain rate imaging of the right ventricular free wall in a pulmonary hypertension patient using tissue Doppler techniques (*A*) and speckle-tracking techniques (*B*).

showed, using a two-segment model, that values for myocardial deformation parameters in the RV free wall are lower in the pulmonary hypertension population when compared with normal controls. Another interesting finding of this study was the heterogeneity in the distribution of S and SR in patients with PH, with lower apical when compared with basal values, and also in the correlations between studied parameters, the values for S and SR in the apical segment correlating strongly with the invasive haemodynamic data.

Another technique that can be employed for determining regional deformation is speckle-tracking-based myocardial deformation imaging. It is advantageous against Doppler techniques as it is relatively angle-independent, and the user-friendly software enables a shorter learning curve. On the other hand, there is a need for excellent image quality when using speckle-tracking-based methods, endocardial border delineation being of most importance for the curve-extracting algorithm, which can be a limitation for the RV study. Teske *et al.*[94] compared values for myocardial deformation parameters using the two methods (TDI and speckle tracking) and showed that they correlate moderately, with TDI values being slightly higher than speckle-tracking-derived values. The feasibility of the two techniques was comparable, both techniques being able to discriminate between physiological and pathological conditions.

Assessing RV regional function has proved valuable in the evaluation of patients with ARVC, with 79% of patients showing regional wall motion abnormalities.[36] Teske *et al.*[39] found that both TDI and 2D strain-derived parameters are superior to conventional echocardiographic parameters in identifying ARVC. Doppler-derived strain in the RV free wall, with a cutoff value of −18.2%, was the best single quantitative echocardiographic parameter to detect RV pathology in patients with known ARVC.

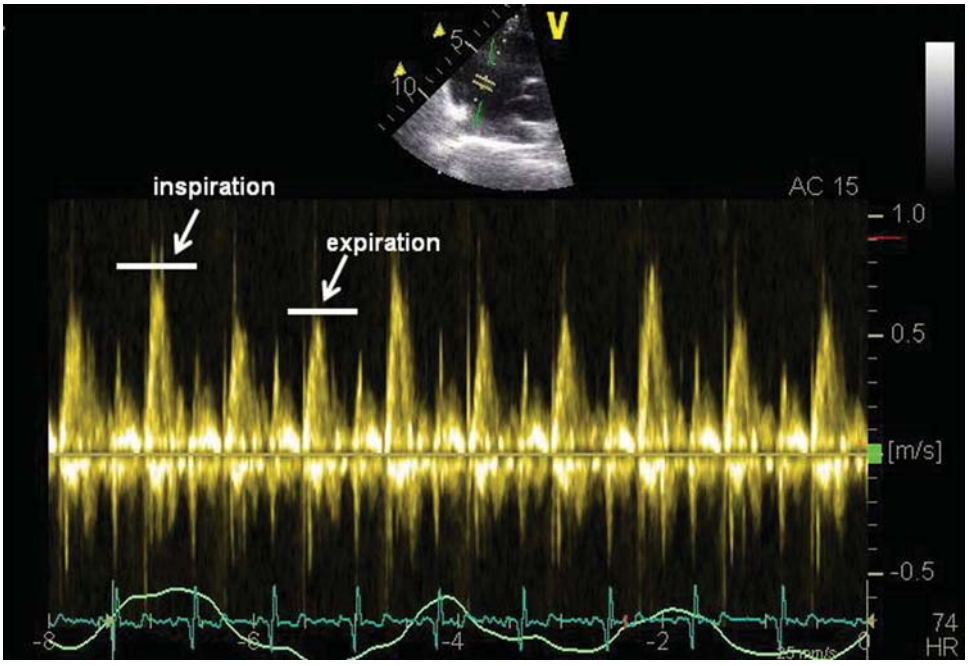

Figure 12 Normal respiratory variations of the tricuspid inflow velocities.

Whether myocardial deformation parameters derived from the RV have added value in daily clinical routine remains a question to be answered, especially given that only small populations have been investigated and normal values are yet to be established.

Visual assessment of RV regional function has proved useful in the diagnosis of patients with PE. McConnell *et al.*[95] described a specific pattern of RV dysfunction in patients with PE, with severe hypokinesia of the mid and basal segments of the RV free wall and hyperkinesia of the apical portion of the same wall. The specificity and sensitivity of this sign for diagnosing PE were 77 and 94%, respectively. However, when validated against helical CT diagnosis of PE, the sensitivity of the McConnell sign was very poor (16%) even if with a high specificity (96%).[96] Moreover, Casazza *et al.* showed that regional free RV wall dysfunction was similar in acute PE and RV infarction.[97,98]

Right ventricular diastolic function

Several echocardiographic parameters can be determined for evaluating RV diastolic function, but less data exist regarding their accuracy.

The tricuspid inflow pattern is obtained in a four-chamber view by placing a cursor at the tips of the tricuspid valve. It is similar to the mitral pattern, although velocities are smaller and there are marked inspiratory variations (*Figure 12*).[99]

The transhepatic flow in a normal individual is characterized by the presence of the three waves: S, D, and A, the latter corresponding to atrial contraction. The fraction of hepatic flow measured as time-velocity integrals (TVIs) of the S and D waves: TVI S/(TVI S + TVI D) was shown to correlate with RA pressures. Furthermore, values below 55% predict an RA pressure of above 8 mmHg with good sensitivity and specificity. Nagueh *et al.*[100] showed that hepatic venous flow dynamics relate best among several parameters (e.g. tricuspid flow, hepatic flow, and inferior vena caval diameters) to mean RA pressure and can be used clinically to estimate mean RA pressure.

Estimation of RA pressure is most often done by assessing the IVC diameter and its degree of collapse with inspiration.[13]

TDI was also employed in analysing diastolic function in the RV. Using the ratio between the tricuspid flow early diastolic velocity (E) and peak early diastolic velocity of the lateral tricuspid annulus (E'), the E/E' ratio was found to have a good correlation with mean invasively measured RA pressure ($r = 0.75$; $P<0.001$). An $E/E' > 6$ had a sensitivity of 79% and a specificity of 73% to detect an RA pressure >10 mmHg.[101]

Conclusions

For many years, the echocardiographic quantitative assessment of RV function has been difficult owing to the complex RV anatomy. Identifying an accurate and reliable echocardiographic parameter for the functional assessment of the RV still remains a challenge. Myocardial velocity and strain rate imaging have promising results in the assessment of RV function. In *Table 2*, we present a summary of the most studied and presently used parameters of RV function, with their reported normal values, as well as advantages and limitations of use. Combinations of these parameters are used in daily clinical practice, each one offering only partial information about the status of the RV. There is hope that novel myocardial deformation parameters and 3D Echo-derived parameters may add value to the examination of the RV, but validation studies are still needed.

Table 2 Normal values for parameters of right ventricular morphology and function

Parameter	Normal values (range or mean ± SD)	Clinical significance	Limitations	Source	Population size	Population age (range or mean ± SD)
RVOT EDD PLAX ($RVOT_1$) (mm)	22 ± 1.5	Diagnosis of patients with ARVD/C		Foale *et al.*[32]	41	19–46
RVOT EDD above aortic valve ($RVOT_2$) (mm)	27 ± 1	Diagnosis of patients with ARVD/C Diagnosis of patients with familial amyloidotic polyneuropathy	Risk of erroneous measurement in oblique sections	Foale *et al.*[32]	41	19–46
RVOT EDD above pulmonary valve ($RVOT_3$) (mm)	20 ± 1.5	Diagnosis of patients with ARVD/C	Risk of erroneous measurement in oblique sections	Foale *et al.*[32]	41	19–46
RVOT SF (%)	61 ± 13	Evaluation of patients with right ventricular failure	Same as measuring diameters; Must be used in combination with RV inflow functional parameters	Lindqvist *et al.*[45]	20	46 ± 12
LV eccentricity index	1	Can be used for separating between RV volume overload and RV pressure overload	Risk of inaccuracies when measuring in oblique sections	Ryan *et al.*[35]	12	36 ± 7
RV wall thickness (mm)	3–5	Diagnosis of RV hypertrophy Good correlation with systolic pulmonary artery pressure	Variability in measurement owing to trabeculations	Foale *et al.*[32] Matsukubo *et al.*[14]	42 25	19–46 17–58
RV inflow EDD (RVIT) (mm)	24 ± 2	Diagnosis of RV dilation	Variability in measurement owing to trabeculations	Foale *et al.*[32]	41	19–46
RV EDA (cm^2)	18 ± 5	Diagnosis of RV dilation	Risk of inaccuracies owing to foreshortened apical four-chamber view Variability in measurement owing to trabeculations and the presence of the moderator band	Lopez-Candales *et al.*[102]	82	50 ± 16
RV ESA (cm^2)	8 ± 4	Diagnosis of RV dilation	Risk of inaccuracies owing to foreshortened apical four-chamber view Variability in measurement owing to trabeculations and the presence of the moderator band	Lopez-Candales *et al.* [102]	82	50 ± 16
RVFAC (%)	56 ± 13	Diagnosis of RV dysfunction Good correlation with RVEF Prognostic value in myocardial infarction and pulmonary hypertension	Same as measuring areas Load-dependent Does not offer information about the inflow region	Lopez-Candales *et al.*[102]	82	50 ± 16
TAPSE (mm)	>15	Simple and easy to measure	Offers information only about longitudinal function	Samad *et al.*[52]	24	63 ± 8
	20 ± 2.8	Good correlation with RVEF Prognostic value in patients with myocardial infarction and patients with pulmonary hypertension	Influenced by the overall movement of the heart	Kukulski *et al.*[81]	32	40 ± 16

Continued

Table 2 *Continued*

Parameter	Normal values (range or mean ± SD)	Clinical significance	Limitations	Source	Population size	Population age (range or mean ± SD)
RV MPI	0.28 ± 0.04	Not limited by RV geometry Evaluation of patients with congenital heart disease and pulmonary hypertension Prognostic value in pulmonary hypertension	Pseudonormalization in the settings of increased atrial pressure Isovolumic periods are less defined in a normal RV	Tei *et al.*[56]	37	43 ± 13
IVA (m/s^2)	1.8 ± 0.6	Relatively load-independent Not limited by RV geometry Evaluation of patients with congenital heart disease	Further clinical validation still needed	Vogel *et al.*[74]	55	22 (mean age)
S_t (cm/s)	Basal: >12	Simple measure Diagnosis of patients with RV myocardial infarction	Angle dependency Offers information only about longitudinal function Influenced by the overall movement of the heart	Meluzin *et al.*[63] Kukulski *et al.*[81] Lindqvist *et al.*[99]	30 32 255	20–74 16–76 22–89
Strain (%)	Basal: 19 ± 6 Mid: 27 ± 6 Apical: 32 ± 6	Offers information about regional function Correlates with RVEF Evaluation of patients with PH	Angle dependency of the measurement (for TDI) High variability in measurements Further clinical validation still needed	Kowalski *et al.*[86]	40	20–42
Strain rate (1/s)	Basal: 1.5 ± 0.4 Mid: 1.72 ± 0.27 Apical: 2.04 ± 0.41	Offers information about regional function Correlates well with contractility Evaluation of patients with PH	Same as strain	Kowalski *et al.*[86]	40	20–42
E (cm/s)	43 ± 11	Evaluation of RV diastolic function	High variability with respiration Dependent on the placement of the sample volume relative to tips of the tricuspid valve	Lindqvist *et al.*[99]	255	22–89
A (cm/s)	31 ± 10	Evaluation of RV diastolic function	Same as E wave	Lindqvist *et al.*[99]	255	22–89
E_t (cm/s)	Basal: 14.5 ± 3.5	Evaluation of RV diastolic dysfunction	Angle dependency of the measurement	Lindqvist *et al.*[99]	255	22–89
E/E_t	>6	Diagnosis of diastolic dysfunction	Same as *E* and E_t The existence of a 'grey zone'	Nageh *et al.*[101]	62	36–90

See text for abbreviations.

Acknowledgements

The authors thank Dr Ciprian Jurcut for technical support with original drawings.

Conflict of interest: J.U.V. has Research Supports and/or Speakers Honoraria from GE, Siemens, Philips, Toshiba, Aloka.

Funding

This work was partially supported by the Romanian National Research Programme II, grant ID_246/2008.

References

1. La Gerche A, Connelly KA, Mooney DJ, MacIsaac AI, Prior DL. Biochemical and functional abnormalities of left and right ventricular function after ultra-endurance exercise. *Heart* 2008;**94**:860–6.
2. Davlouros PA, Niwa K, Webb G, Gatzoulis MA. The right ventricle in congenital heart disease. *Heart* 2006;**92**:i27–i38.
3. Voelkel NF, Quaife RA, Leinwand LA, Barst RJ, McGoon MD, Meldrum DR *et al.* Right ventricular function and failure: Report of a National Heart, Lung, and Blood Institute Working Group on Cellular and Molecular Mechanisms of Right Heart Failure. *Circulation* 2006;**114**:1883–91.
4. D'Alonzo GE, Barst RJ, Ayres SM, Bergofsky EH, Brundage BH, Detre KM *et al.* Survival in patients with primary pulmonary hypertension: results from a national prospective registry. *Ann Intern Med* 1991;**115**:343–9.
5. Juilliere Y, Barbier G, Feldmann L, Grentzinger A, Danchin N, Cherrier F. Additional predictive value of both left and right ventricular ejection fractions on long-term survival in idiopathic dilated cardiomyopathy. *Eur Heart J* 1997;**18**:276–80.
6. Chin KM, Kim NH, Rubin LJ. The right ventricle in pulmonary hypertension. *Coron Artery Dis* 2005;**16**:13–8.
7. Anderson RH, Razavi R, Taylor AM. Cardiac anatomy revisited. *J Anat* 2004;**205**:159–77.
8. Bodhey NK, Beerbaum P, Sarikouch S, Kropf S, Lange P, Berger F *et al.* Functional analysis of the components of the right ventricle in the setting of tetralogy of Fallot. *Circ Cardiovasc Imaging* 2008;**1**:141–7.
9. Anderson RH, Smerup M, Sanchez-Quintana D, Loukas M, Lunkenheimer PP. The three-dimensional arrangement of the myocytes in the ventricular walls. *Clin Anat* 2009;**22**:64–76.
10. Leather HA, Ama' R, Missant C, Rex S, Rademakers FE, Wouters PF. Longitudinal but not circumferential deformation reflects global contractile function in the right ventricle with open pericardium. *Am J Physiol Heart Circ Physiol* 2006;**290**:H2369–H2375.
11. Kukulski T, Hubbert L, Arnold M, Wranne B, Hatle L, Sutherland GR. Normal regional right ventricular function and its change with age: a Doppler myocardial imaging study. *J Am Soc Echocardiogr* 2000;**13**:194–204.
12. Meier GD, Bove AA, Santamore WP, Lynch PR. Contractile function in canine right ventricle. *Am J Physiol Heart Circ Physiol* 1980;**239**:H794–H804.
13. Lang RM, Bierig M, Devereux RB, Flachskampf FA, Foster E, Pellikka PA *et al.* Recommendations for chamber quantification. *Eur J Echocardiogr* 2006;**7**:79–108.
14. Matsukubo H, Matsuura T, Endo N, Asayama J, Watanabe T. Echocardiographic measurement of right ventricular wall thickness. A new application of subxiphoid echocardiography. *Circulation* 1977;**56**:278–84.
15. Sandstede J, Lipke C, Beer M, Hofmann S, Pabst T, Kenn W *et al.* Age- and gender-specific differences in left and right ventricular cardiac function and mass determined by cine magnetic resonance imaging. *Eur Radiol* 2000;**10**:438–42.
16. Maceira AM, Prasad SK, Khan M, Pennell DJ. Reference right ventricular systolic and diastolic function normalized to age, gender and body surface area from steady-state free precession cardiovascular magnetic resonance. *Eur Heart J* 2006;**27**:2879–2888.
17. Opie L. Mechanisms of cardiac contraction and relaxation. In: Braunwald E, Bonow R, Mann D, Zipes D, Libby T, eds., *Braunwald's Heart Diseases. A textbook of Cardiovascular Medicine.* 8th ed. Elsevier; 2008. p509–39.
18. Sheehan F, Redington A. The right ventricle: anatomy, physiology and clinical imaging. *Heart* 2008;**94**:1510–5.
19. Santamore WP, Dell'italia LJ. Ventricular interdependence: significant left ventricular contributions to right ventricular systolic function. *Prog Cardiovasc Dis* 1998;**40**:289–308.
20. Yamaguchi S, Harasawa H, Li KS, Zhu D, Santamore WP. Comparative significance in systolic ventricular interaction. *Cardiovasc Res* 1991;**25**:774–83.
21. Hoffman D, Sisto D, Frater RWM, Nikolic SD. Left-to-right ventricular interaction with a noncontracting right ventricle. *J Thorac Cardiovasc Surg* 1994;**107**:1496–502.
22. Redington AN, Rigby ML, Shinebourne EA, Oldershaw PJ. Changes in the pressure–volume relation of the right ventricle when its loading conditions are modified. *Br Heart J* 1990;**63**:45–9.
23. Redington AN, Gray HH, Hodson ME, Rigby ML, Oldershaw PJ. Characterisation of the normal right ventricular pressure–volume relation by biplane angiography and simultaneous micromanometer pressure measurements. *Br Heart J* 1988;**59**:23–30.
24. Shaver JA, Nadolny RA, O'Toole JD, Thompson ME, Reddy PS, Leon DF *et al.* Sound pressure correlates of the second heart sound: an intracardiac sound study. *Circulation* 1974;**49**:316–25.
25. O'Rourke RA, Dell'Italia LJ. Diagnosis and management of right ventricular myocardial infarction. *Curr Probl Cardiol* 2004;**29**:6–47.
26. Lindstrom L, Wilkenshoff UM, Larsson H, Wranne B. Echocardiographic assessment of arrhythmogenic right ventricular cardiomyopathy. *Heart* 2001;**86**:31–8.
27. Goldhaber SZ. Pulmonary embolism. *Lancet* 2004;**363**:1295–305.
28. Belik J, Light RB. Effect of increased afterload on right ventricular function in newborn pigs. *J Appl Physiol* 1989;**66**:863–9.
29. Lurz P, Puranik R, Nordmeyer J, Muthurangu V, Hansen MS, Schievano S *et al.* Improvement in left ventricular filling properties after relief of right ventricle to pulmonary artery conduit obstruction: contribution of septal motion and interventricular mechanical delay. *Eur Heart J* 2009;**30**:2266–74.
30. Greil GF, Beerbaum P, Razavi R, Miller O. Imaging the right ventricle: non-invasive imaging. *Heart* 2008;**94**:803–8.
31. Ho SY, Nihoyannopoulos P. Anatomy, echocardiography, and normal right ventricular dimensions. *Heart* 2006;**92**:i2–i13.
32. Foale R, Nihoyannopoulos P, McKenna W, Kleinebenne A, Nadazdin A, Rowland E *et al.* Echocardiographic measurement of the normal adult right ventricle. *Br Heart J* 1986;**56**:33–44.
33. Haddad F, Hunt SA, Rosenthal DN, Murphy DJ. Right ventricular function in cardiovascular disease, part I. Anatomy, physiology, aging, and functional assessment of the right ventricle. *Circulation* 2008;**117**:1436–48.
34. Feigenbaum H, Armstrong W, Ryan T. Left atrium, right atrium, right ventricle. In: Feigenbaum H, Armstrong W, Ryan T, eds. *Feigenbaum's Echocardiography.* Lippincott Williams &Wilkins; 2005. p. 181–213.
35. Ryan T, Petrovic O, Dillon JC, Feigenbaum H, Conley MJ, Armstrong WF. An echocardiographic index for separation of right ventricular volume and pressure overload. *J Am Coll Cardiol* 1985;**5**:918–27.
36. Yoerger DM, Marcus F, Sherrill D, Calkins H, Towbin JA, Zareba W *et al.* Echocardiographic findings in patients meeting task force criteria for arrhythmogenic right ventricular dysplasia: new insights from the multidisciplinary study of right ventricular dysplasia. *J Am Coll Cardiol* 2005;**45**:860–5.
37. Kaul S, Tei C, Hopkins JM, Shah PM. Assessment of right ventricular function using two-dimensional echocardiography. *Am Heart J* 1984;**107**:526–31.
38. Frances RJ. Arrhythmogenic right ventricular dysplasia/cardiomyopathy. A review and update. *Int J Cardiol* 2006;**110**:279–87.
39. Teske AJ, Cox MG, De Boeck BW, Doevendans PA, Hauer RN, Cramer MJ. Echocardiographic tissue deformation imaging quantifies abnormal regional right ventricular function in arrhythmogenic right ventricular dysplasia/cardiomyopathy. *J Am Soc Echocardiogr* 2009;**22**:920–7.
40. Gopal AS, Chukwu EO, Iwuchukwu CJ, Katz AS, Toole RS, Schapiro W *et al.* Normal values of right ventricular size and function by real-time 3-dimensional echocardiography: comparison with cardiac magnetic resonance imaging. *J Am Soc Echocardiogr* 2007;**20**:445–55.
41. Shiota T. 3D echocardiography: evaluation of the right ventricle. *Curr Opin Cardiol* 2009;**24**:410–414.
42. Sechtem U, Pflugfelder PW, Gould RG, Cassidy MM, Higgins CB. Measurement of right and left ventricular volumes in healthy individuals with cine MR imaging. *Radiology* 1987;**163**:697–702.
43. Grothues F, Smith GC, Moon JCC, Bellenger NG, Collins P, Klein HU *et al.* Comparison of interstudy reproducibility of cardiovascular magnetic resonance with two-dimensional echocardiography in normal subjects and in patients with heart failure or left ventricular hypertrophy. *Am J Cardiol* 2002;**90**:29–34.
44. Lindqvist P, Calcutteea A, Henein M. Echocardiography in the assessment of right heart function. *Eur J Echocardiogr* 2008;**9**:225–34.
45. Lindqvist P, Henein M, Kazzam E. Right ventricular outflow-tract fractional shortening: an applicable measure of right ventricular systolic function. *Eur J Echocardiogr* 2003;**4**:29–35.
46. Zornoff LAM, Skali H, Pfeffer MA, John Sutton M, Rouleau JL, Lamas GA *et al.* Right ventricular dysfunction and risk of heart failure and mortality after myocardial infarction. *J Am Coll Cardiol* 2002;**39**:1450–5.

47. Ghio S, Gavazzi A, Campana C, Inserra C, Klersy C, Sebastiani R *et al.* Independent and additive prognostic value of right ventricular systolic function and pulmonary artery pressure in patients with chronic heart failure. *J Am Coll Cardiol* 2001;**37**:183–8.
48. Anavekar NS, Skali H, Bourgoun M, Ghali JK, Kober L, Maggioni AP *et al.* Usefulness of right ventricular fractional area change to predict death, heart failure, and stroke following myocardial infarction (from the VALIANT ECHO study). *Am J Cardiol* 2008;**101**:607–12.
49. Anavekar NS, Gerson D, Skali H, Kwong RY, Yucel EK, Solomon SD. Two-dimensional assessment of right ventricular function: an echocardiographic-MRI correlative study. *Echocardiography* 2007;**24**:452–6.
50. Karatasakis GT, Karagounis LA, Kalyvas PA, Manginas A, Athanassopoulos GD, Aggelakas SA *et al.* Prognostic significance of echocardiographically estimated right ventricular shortening in advanced heart failure. *Am J Cardiol* 1998;**82**: 329–34.
51. Goldberger JJ, Himelman RB, Wolfe CL, Schiller NB. Right ventricular infarction: recognition and assessment of its hemodynamic significance by two-dimensional echocardiography. *J Am Soc Echocardiogr* 1991;**4**:140–6.
52. Samad BA, Alam M, Jensen-Urstad K. Prognostic impact of right ventricular involvement as assessed by tricuspid annular motion in patients with acute myocardial infarction. *Am J Cardiol* 2002;**90**:778–81.
53. Coghlan JG, Davar J. How should we assess right ventricular function in 2008? *Eur Heart J Suppl* 2007;**9**:H22–8.
54. Lopez-Candales A, Rajagopalan N, Saxena N, Gulyasy B, Edelman K, Bazaz R. Right ventricular systolic function is not the sole determinant of tricuspid annular motion. *Am J Cardiol* 2006;**98**:973–7.
55. Giusca S, Dambrauskaite V, Scheurwegs C, D'hooge J, Claus P, Herbots L *et al.* Deformation imaging describes RV function better than longitudinal displacement of the tricuspid ring (TAPSE). *Heart* 2010; doi:10.1136/hrt.2009.171728.
56. Tei C, Dujardin KS, Hodge DO, Bailey KR, McGoon MD, Tajik AJ *et al.* Doppler echocardiographic index for assessment of global right ventricular function. *J Am Soc Echocardiogr* 1996;**9**:838–47.
57. Karnati PK, El-Hajjar M, Torosoff M, Fein SA. Myocardial performance index correlates with right ventricular ejection fraction measured by nuclear ventriculography. *Echocardiography* 2008;**25**:381–5.
58. Tei C, Dujardin KS, Hodge DO, Bailey KR, McGoon MD, Tajik AJ *et al.* Doppler echocardiographic index for assessment of global right ventricular function. *J Am SocEchocardiogr* 1996;**9**:838–47.
59. Blanchard DG, Malouf PJ, Gurudevan SV, Auger WR, Madani MM, Thistlethwaite P *et al.* Utility of right ventricular Tei index in the noninvasive evaluation of chronic thromboembolic pulmonary hypertension before and after pulmonary thromboendarterectomy. *J Am Coll Cardiol Img* 2009;**2**:143–9.
60. Menzel T, Kramm T, Mohr-Kahaly S, Mayer E, Oelert H, Meyer J. Assessment of cardiac performance using Tei indices in patients undergoing pulmonary thromboendarterectomy. *Ann Thorac Surg* 2002;**73**:762–6.
61. Yoshifuku S, Otsuji Y, Takasaki K, Yuge K, Kisanuki A, Toyonaga K *et al.* Pseudonormalized Doppler total ejection isovolume (Tei) index in patients with right ventricular acute myocardial infarction. *Am J Cardiol* 2003;**91**:527–31.
62. Stein PD, Sabbah HN, Anbe DT, Marzilli M. Performance of the failing and nonfailing right ventricle of patients with pulmonary hypertension. *Am J Cardiol* 1979; **44**:1050–5.
63. Meluzin J, Spinarova L, Bakala J, Toman J, Krejci J, Hude P *et al.* Pulsed Doppler tissue imaging of the velocity of tricuspid annular systolic motion. A new, rapid, and non-invasive method of evaluating right ventricular systolic function. *Eur Heart J* 2001;**22**:340–8.
64. Kukulski T, Voigt JU, Wilkenshoff UM, Strotmann JM, Wranne B, Hatle L *et al.* A comparison of regional myocardial velocity information derived by pulsed and color Doppler techniques: an *in vitro* and *in vivo* study. *Echocardiography* 2000;**17**:639–51.
65. Lind B, Nowak J, Dorph J, van der Linden J, Brodin LA. Analysis of temporal requirements for myocardial tissue velocity imaging. *Eur J Echocardiogr* 2002;**3**: 214–9.
66. Triffon D, Groves BM, Reeves JT, Ditchey RV. Determinants of the relation between systolic pressure and duration of isovolumic relaxation in the right ventricle. *J Am Coll Cardiol* 1988;**11**:322–9.
67. Sutherland GR, Kowalski M, Kukulski T, Ionescu A. The right ventricle. In: Sutherland GR, Hatle L, Claus P, D'hooge J, Bijnens B, eds. *Doppler Myocardial Imaging.* BSWK, Belgium, 2006. p309–24.
68. Gondi S, Dokainish H. Right ventricular tissue Doppler and strain imaging: ready for clinical use? *Echocardiography* 2007;**24**:522–32.
69. Harada K, Tamura M, Toyono M, Yasuoka K. Comparison of the right ventricular Tei index by tissue Doppler imaging to that obtained by pulsed Doppler in children without heart disease. *Am J Cardiol* 2002;**90**:566–9.
70. Hsiao SH, Wang WC, Yang SH, Lee CY, Chang SM, Lin SK *et al.* Myocardial tissue Doppler-based indexes to distinguish right ventricular volume overload from right ventricular pressure overload. *Am J Cardiol* 2008;**101**: 536–41.
71. Vogel M, Schmidt MR, Kristiansen SB, Cheung M, White PA, Sorensen K *et al.* Validation of myocardial acceleration during isovolumic contraction as a novel noninvasive index of right ventricular contractility: comparison with ventricular pressure–volume relations in an animal model. *Circulation* 2002;**105**: 1693–9.
72. Kjaergaard J, Snyder EM, Hassager C, Oh JK, Johnson BD. Impact of preload and afterload on global and regional right ventricular function and pressure: a quantitative echocardiography study. *J Am Soc Echocardiogr* 2006;**19**:515–21.
73. Bleeker GB, Holman ER, Abraham T, Bax JJ. Tissue Doppler imaging and strain rate imaging to evaluate right ventricular function. In: Yu CM, Marwick T, eds. *Myocardial Imaging: Tissue Doppler and Speckle Tracking.* Wiley-Blackwell, 2007. p243–51.
74. Vogel M, Derrick G, White PA, Cullen S, Aichner H, Deanfield J *et al.* Systemic ventricular function in patients with transposition of the great arteries after atrial repair: a tissue Doppler and conductance catheter study. *J Am Coll Cardiol* 2004; **43**:100–6.
75. Frigiola A, Redington AN, Cullen S, Vogel M. Pulmonary regurgitation is an important determinant of right ventricular contractile dysfunction in patients with surgically repaired tetralogy of Fallot. *Circulation* 2004;**110**:II-153–7.
76. Lyseggen E, Rabben SI, Skulstad H, Urheim S, Risoe C, Smiseth OA. Myocardial acceleration during isovolumic contraction: relationship to contractility. *Circulation* 2005;**111**:1362–9.
77. Kjaergaard J, Petersen CL, Kjaer A, Schaadt BK, Oh JK, Hassager C. Evaluation of right ventricular volume and function by 2D and 3D echocardiography compared to MRI. *Eur J Echocardiogr* 2006;**7**:430–8.
78. Jenkins C, Chan J, Bricknell K, Strudwick M, Marwick TH. Reproducibility of right ventricular volumes and ejection fraction using real-time three-dimensional echocardiography: comparison with cardiac MRI. *Chest* 2007;**131**:1844–51.
79. Niemann PS, Pinho L, Balbach T, Galuschky C, Blankenhagen M, Silberbach M *et al.* Anatomically oriented right ventricular volume measurements with dynamic three-dimensional echocardiography validated by 3-tesla magnetic resonance imaging. *J Am Coll Cardiol* 2007;**50**:1668–76.
80. Lu X, Nadvoretskiy V, Bu L, Stolpen A, Ayres N, Pignatelli RH *et al.* Accuracy and reproducibility of real-time three-dimensional echocardiography for assessment of right ventricular volumes and ejection fraction in children. *J Am Soc Echocardiogr* 2008;**21**:84–9.
81. Kukulski T, Hnbbert L, Arnold M, Wranne B, Hatle L, Sutherland GR. Normal regional right ventricular function and its change with age: a Doppler myocardial imaging study. *J Am Soc Echocardiogr* 2000;**13**:194–204.
82. Dambrauskaite V, Delcroix M, Claus P, Herbots L, D'hooge J, Bijnens B *et al.* Regional right ventricular dysfunction in chronic pulmonary hypertension. *J Am Soc Echocardiogr* 2007;**20**:1172–80.
83. Greaves K, Puranik R, O'Leary JJ, Celermajer DS. Myocardial tissue velocities in the normal left and right ventricle: relationships and predictors. *Heart Lung Circ* 2004;**13**:367–73.
84. Dokainish H, Abbey H, Gin K, Ramanathan K, Lee PK, Jue J. Usefulness of tissue Doppler imaging in the diagnosis and prognosis of acute right ventricular infarction with inferior wall acute left ventricular infarction. *Am J Cardiol* 2005; **95**:1039–42.
85. Sutherland GR, Di Salvo G, Claus P, D'hooge J, Bijnens B. Strain and strain rate imaging: a new clinical approach to quantifying regional myocardial function. *J Am Soc Echocardiogr* 2004;**17**:788–802.
86. Kowalski M, Kukulski T, Jamal F, D'hooge J, Weidemann F, Rademakers F *et al.* Can natural strain and strain rate quantify regional myocardial deformation? A study in healthy subjects. *Ultrasound Med Biol* 2001;**27**:1087–97.
87. Weidemann F, Kowalski M, D'hooge J, Bijnens B, Sutherland GR. Doppler myocardial imaging. A new tool to assess regional inhomogeneity in cardiac function. *Basic Res Cardiol* 2001;**96**:595–605.
88. Jurcut R, Wildiers H, Ganame J, D'hooge J, Paridaens R, Voigt JU. Detection and monitoring of cardiotoxicity—what does modern cardiology offer? *Support Care Cancer* 2008;**16**:437–45.
89. Voigt JU, Exner B, Schmiedehausen K, Huchzermeyer C, Reulbach U, Nixdorff U *et al.* Strain-rate imaging during dobutamine stress echocardiography provides objective evidence of inducible ischemia. *Circulation* 2003;**107**:2120–6.
90. Weidemann F, Jamal F, Sutherland GR, Claus P, Kowalski M, Hatle L *et al.* Myocardial function defined by strain rate and strain during alterations in inotropic states and heart rate. *Am J Physiol Heart Circ Physiol* 2002;**283**:H792–9.
91. Greenberg NL, Firstenberg MS, Castro PL, Main M, Travaglini A, Odabashian JA *et al.* Doppler-derived myocardial systolic strain rate is a strong index of left ventricular contractility. *Circulation* 2002;**105**:99–105.
92. Teske AJ, Prakken NH, De Boeck BW, Velthuis BK, Martens EP, Doevendans PA *et al.* Echocardiographic tissue deformation imaging of right ventricular systolic function in endurance athletes. *Eur Heart J* 2009;**30**:969–77.

93. Huez S, Vachiery JL, Unger P, Brimioulle S, Naeije R. Tissue Doppler imaging evaluation of cardiac adaptation to severe pulmonary hypertension. *Am J Cardiol* 2007;**100**:1473–8.
94. Teske AJ, De Boeck BWL, Olimulder M, Prakken NH, Doevendans PAF, Cramer MJ. Echocardiographic assessment of regional right ventricular function: a head-to-head comparison between 2-dimensional and tissue Doppler-derived strain analysis. *J Am Soc Echocardiogr* 2008;**21**:275–83.
95. McConnell MV, Solomon SD, Rayan ME, Come PC, Goldhaber SZ, Lee RT. Regional right ventricular dysfunction detected by echocardiography in acute pulmonary embolism. *Am J Cardiol* 1996;**78**:469–73.
96. Lodato JA, Ward RP, Lang RM. Echocardiographic predictors of pulmonary embolism in patients referred for helical CT. *Echocardiography* 2008;**25**: 584–90.
97. Casazza F, Bongarzoni A, Capozi A, Agostoni O. Regional right ventricular dysfunction in acute pulmonary embolism and right ventricular infarction. *Eur J Echocardiogr* 2005;**6**:11–4.
98. Torbicki A. Echocardiographic diagnosis of pulmonary embolism: a rise and fall of McConnell sign? *Eur J Echocardiogr* 2005;**6**:2–3.
99. Lindqvist P, Waldenstrom A, Henein M, Morner S, Kazzam E. Regional and global right ventricular function in healthy individuals aged 20–90 years: a pulsed Doppler tissue imaging study: Umea General Population Heart Study. *Echocardiography* 2005;**22**:305–14.
100. Nagueh SF, Kopelen HA, Zoghbi WA. Relation of mean right atrial pressure to echocardiographic and Doppler parameters of right atrial and right ventricular function. *Circulation* 1996;**93**:1160–9.
101. Nageh MF, Kopelen HA, Zoghbi WA, Quinones MA, Nagueh SF. Estimation of mean right atrial pressure using tissue Doppler imaging. *Am J Cardiol* 1999;**84**: 1448–51.
102. Lopez-Candales A, Dohi K, Rajagopalan N, Edelman K, Gulyasy B, Bazaz R. Defining normal variables of right ventricular size and function in pulmonary hypertension: an echocardiographic study. *Postgrad Med J* 2008;**84**: 40–5.